This article has been accepted for publication in a future issue of this journal, but has not been fully edited. Content may change prior to final publication. Citation information: DOI 10.1109/LWC.2019.2939305, IEEE Wireless Communications Letters

Multi-cell MMSE Combining over Correlated Rician Channels in Massive MIMO Systems

Ikram Boukhedimi, Abla Kammoun, and Mohamed-Slim Alouini
Computer, Electrical, and Mathematical Sciences and Engineering (CEMSE) Division,
King Abdullah University of Science and Technology (KAUST),
Thuwal, Makkah Province, Kingdom of Saudi Arabia.
Email: {ikram.boukhedimi, abla.kammoun, slim.alouini}@kaust.edu.sa

***Abstract*—This work investigates the uplink of massive MIMO systems using multi-cell MMSE (M-MMSE) combining that was shown to yield unbounded capacity in Rayleigh fading. All intra and inter-cell channels are correlated with distinct per-user Rician factors and channel correlation matrices, pilot contamination and imperfect channel estimation. First, a closed-form approximation of the spectral efficiency (SE) is derived thus enabling to demonstrate that, under certain conditions on the correlation matrices, M-MMSE generates unbounded SE in Rician fading. Second, the impact of inter-cell LoS components is examined in favorable propagation conditions, and, interestingly, shown to be more beneficial in terms of SE than when these interfering links are entirely scattered.**

***Index Terms*—Massive MIMO, M-MMSE, unlimited capacity, correlated Rician fading, pilot contamination, inter-cell LoS.**

I. Introduction

By using a large number of antennas, and performing efficient spatial multiplexing, massive MIMO can generate scalable ergodic capacities through fairly simple linear processing techniques [1]. Despite the substantial advantages of massive MIMO, many issues remain to be tackled. In multi-cell networks, studies have shown that interference emanating from pilot contamination is a major impediment that limits the achievable capacity [2]. Interestingly, the authors in [3] show that by utilizing estimates of all interfering channels, multi-cell MMSE (M-MMSE) combining mitigates both intra and inter-cell interference, and therefore yields a spectral efficiency (SE) that scales with the number of antennas. This work, however, considers Rayleigh fading which does not encompass Line-of-Sight (LoS) components. On the other hand, in [4], the authors investigate single-cell combining schemes and show that interference generated by pilot contamination decreases as the LoS signals become stronger. Therefore, it is paramount to investigate M-MMSE when the system involves both LoS and NLoS signals which calls for Rician fading.

Examining the performance of massive MIMO over Rician fading channels has received a lot of interest (see [4]–[9] and references therein). Among these, only a few study the multi-cell setting with pilot contamination [4], [7], [8]; however with either uncorrelated channels, single-cell detection techniques, or only intra-LoS channels. Accordingly, in this work we consider a more general system model wherein every channel (including the inter-cell links) accounts for a distinct Rician factor and correlation matrix, in addition to pilot contamination and imperfect channel state information (CSI). Such a setting is quite comprehensive and can be useful for the investigation of systems where the probability of both intra-cell and inter-cell LoS signals is prevalent like in heterogeneous networks, emerging UAV aided wireless systems, to name a few.

The analysis is led using an asymptotic approximation of the spectral efficiency which we derive in Section II assuming the infinite antenna regime, and validate in Section III with a selection of numerical results. The study confirms that M-MMSE provides unbounded spectral efficiency even under the presence of intra and inter-LoS interference, thereby extending the results in [3] to Rician fading. Additionally, another key outcome from the analysis shows that settings with inter-cell LoS components generate increasingly higher spectral efficiency gains than when the interfering inter-cell channels are entirely scattered.

II. System Model

Consider the UL of a TDD system operating over a block-flat fading channel with L base stations (BSs). Each BS$_j$ has N_j antennas and is assigned K single-antenna users. Throughout the paper, we consider cell j as cell of interest. Every channel $\mathbf{h}_{j\ell k}$ in the system comprehends a distinct Rician factor $\kappa_{j\ell k}$ and channel correlation matrix $\mathbf{\Theta}_{j\ell k}$, which are assumed to be slowly varying compared to the channel coherence time T_c and hence, supposed to be perfectly known to BS$_j$. Generally, they can be estimated in a previous transmission and averaged over several previous estimation phases (see [10, Section 3.3.3] and references therein) . Accordingly, let $\mathbf{h}_{j\ell k}$ represent the correlated Rician channel linking the $k-$th UE in cell ℓ to BS$_j$ be defined as:

$$\mathbf{h}_{j\ell k} = \mathbf{R}_{j\ell k}^{\frac{1}{2}} \mathbf{z}_{j\ell k} + \overline{\mathbf{h}}_{j\ell k}, \tag{1}$$

where $\mathbf{R}_{j\ell k} = \frac{\beta_{j\ell k}}{1+\kappa_{j\ell k}} \mathbf{\Theta}_{j\ell k}$ with $\beta_{j\ell k}$ is the large-scale fading parameter, $\mathbf{z}_{j\ell k} \sim \mathcal{CN}\left(0, \mathbf{I}_{N_j}\right)$ depicts the scattered (NLoS) signals, and the deterministic quantity $\overline{\mathbf{h}}_{j\ell k} = \sqrt{\frac{\beta_{j\ell k}\kappa_{j\ell k}}{1+\kappa_{j\ell k}}}\ \overline{\mathbf{z}}_{j\ell k}$ with $\overline{\mathbf{z}}_{jk} \in \mathbb{C}^{N_j}$ represents the specular

Notations: In the sequel, $log(.)$ is the natural logarithm, the $N \times N$ identity matrix is denoted $\boldsymbol{I}_N$, and $\mathbf{0}_{N\times K}$ is the $N \times K$ all zeros matrix. Plus, $[\mathbf{A}]_{ij}$ is the element on the $i-$th row and $j-$th column of matrix $\mathbf{A}$, and $diag\left\{a_i\right\}_{i=1}^{N}$ is the $N \times N$ diagonal matrix with a_i being its $i-$th diagonal element. Finally, $\mathcal{B}\left(\mathbf{A}, \ell, j\right)$ refers to the $\ell j-$th block of the block-matrix $\mathbf{A}$.

This article has been accepted for publication in a future issue of this journal, but has not been fully edited. Content may change prior to final publication. Citation information: DOI 10.1109/LWC.2019.2939305, IEEE Wireless Communications Letters

(LoS) links with Rician factor $\kappa_{j\ell k} \geq 0$. Finally, let $\overline{\mathbf{H}}_j = \left[\overline{\mathbf{h}}_{j11} \dots \overline{\mathbf{h}}_{j\ell k} \dots \overline{\mathbf{h}}_{jLK_L}\right]$ denote the aggregate matrix of the LoS components of BS$_j$. In order to estimate the channels, the UEs in each cell transmit mutually orthogonal pilot sequences during a training phase of τ symbols out of the total coherence interval T_c. To account for pilot contamination, we assume pilot reuse in every cell. Formally, we consider that the same pilot is assigned to every k-th UE in each cell, and as such $\forall(j,k)$, the estimates of the channels $\mathbf{h}_{j1k}, \mathbf{h}_{j2k}, \dots, \mathbf{h}_{jLk}$, are correlated. Accordingly, using the MMSE estimation, the estimate of $\mathbf{h}_{j\ell k}$ is given by:

$$\widehat{\mathbf{h}}_{j\ell k} = \mathbf{R}_{j\ell k}\mathbf{\Phi}_{jk}\left(\sum_{\ell'=1}^{L}\mathbf{h}_{j\ell' k} + \frac{1}{\sqrt{\tau\rho}}\mathbf{n}_{jk}^{tr}\right) + \overline{\mathbf{h}}_{j\ell k}, \quad (2)$$

thus, $\widehat{\mathbf{h}}_{j\ell k} \sim \mathcal{CN}\left(\overline{\mathbf{h}}_{jk}, \mathbf{R}_{j\ell k}\mathbf{\Phi}_{jk}\mathbf{R}_{j\ell k}\right)$, where $\mathbf{\Phi}_{jk} = \left(\sum_{\ell'=1}^{L}\mathbf{R}_{j\ell' k} + \frac{1}{\tau\rho_{tr}}\mathbf{I}_{N_j}\right)^{-1}$, with $\rho = \frac{p}{\sigma^2}$ and $\mathbf{n}_{jk}^{tr}$ are, respectively, the SNR and noise during training. In order to retrieve the signal sent by UE k, BS$_j$ uses a linear receiver $\mathbf{g}_{jk} \in \mathbb{C}^{N_j \times 1}$. As previously mentioned, this work investigates the multi-cell MMSE combining design for $\mathbf{g}_{jk}$:

$$\mathbf{g}_{jk} = \left(\sum_{\ell=1}^{L}\sum_{i=1}^{K}\widehat{\mathbf{h}}_{j\ell i}\widehat{\mathbf{h}}_{j\ell i}^{\mathrm{H}} + (\mathbf{Z}_j)^{-1}\right)^{-1}\widehat{\mathbf{h}}_{jjk}, \quad (3)$$

with $(\mathbf{Z}_j)^{-1} = \frac{1}{\rho_d}\mathbf{I}_{N_j} + \sum_{\ell=1}^{L}\sum_{i=1}^{K_\ell}(\mathbf{R}_{j\ell i} - \mathbf{R}_{j\ell i}\mathbf{\Phi}_{ji}\mathbf{R}_{j\ell i})$. Recalling that the M-MMSE vector is obtained through the optimization of the UL SINR, note that its expression in the current system model assuming Rician fading (3) is analogous to that of Rayleigh fading provided in [3] since the optimization problem simply reduces to maximizing a Rayleigh Quotient. Therefore, the derivation of (3) is omitted for space limitations. Accordingly, the UL SINR and the achievable spectral efficiency are, respectively, defined as :

$$\gamma_{jk} = \widehat{\mathbf{h}}_{jjk}^{\mathrm{H}}\left(\sum_{(\ell,i)\neq(j,k)}\widehat{\mathbf{h}}_{j\ell i}\widehat{\mathbf{h}}_{j\ell i}^{\mathrm{H}} + (\mathbf{Z}_j)^{-1}\right)^{-1}\widehat{\mathbf{h}}_{jjk}, \quad (4)$$

$$\mathrm{SE}_{jk} = \left(1 - \frac{\tau}{T_c}\right)\mathbb{E}\left[\log\left(1+\gamma_{jk}\right)\right]. \quad (5)$$

III. Analysis of Achievable UL SE

We derive in this section closed-form deterministic equivalents of the SINR γ_{jk} which, according to the continuous mapping theorem (CMT) [11], leads to an approximation of the UL SE. These approximations, as shall be asserted by simulations, are tight for finite system dimension, and thus provide an analytical framework that is valid for different channel correlation structures and Rician factors. As $N_j \to \infty$, while K is maintained fixed, we consider the following assumptions:

Assumption 1. $\forall j,\ \ell,\ k$,
$\limsup_{N_j}\|\mathbf{R}_{j\ell k}\|_2 < \infty$, *and* $\liminf_{N_j}\frac{1}{N_j}\mathrm{tr}(\mathbf{R}_{j\ell k}) > 0$,
$\limsup_{N_j}\frac{1}{\sqrt{N_j}}\left\|\overline{\mathbf{H}}_{j\ell}\right\|_2 < \infty$, $\liminf_{N_j}\frac{1}{N_j}\mathrm{tr}\left(\overline{\mathbf{H}}_{j\ell}\right) > 0$.

Assumption 2 (Asymptotic linear independence [10])**.** $\forall j,\ell,k$, *with* $\boldsymbol{\lambda}_{jk} = [\lambda_{j1}k, \dots, \lambda_{jLk}]^T$ *and* $\ell' = 1, \dots, L$*:*

$$\liminf_{N_j}\inf_{\{\boldsymbol{\lambda}_{jk}:\lambda_{j\ell' k}=1\}}\frac{1}{N_j}\left\|\sum_{\ell=1}^{L}\lambda_{j\ell k}\mathbf{R}_{j\ell k}\right\|_F^2 > 0.$$

Theorem 1. *Under assumptions 1-2, we have:*

$\frac{1}{N_j}\gamma_{jk} - \frac{1}{N_j}\overline{\gamma}_{jk} \xrightarrow[N\to\infty]{a.s.} 0$, *s.t:*

$$\frac{1}{N_j}\overline{\gamma}_{jk} = \frac{1}{\left[\left(\mathbf{B}_{jk} + \frac{1}{N_j}\overline{\mathbf{H}}_{j,k}^{H}\overline{\mathbf{Q}}_{jk}\overline{\mathbf{H}}_{j,k}\right)^{-1}\right]_{jj}} \quad (6)$$

where $\mathbf{B}_{jk} \in \mathbb{R}^{L\times L}$, *s.t.* $[\mathbf{B}_{jk}]_{mn} = \frac{1}{N_j}\mathrm{tr}\left(\mathbf{R}_{jnk}\mathbf{\Phi}_{jk}\mathbf{R}_{jmk}\mathbf{Z}_j\right)$, *and* $\overline{\mathbf{Q}}_{jk}$ *is a* $N_j \times N_j$ *matrix defined as:*

$$\overline{\mathbf{Q}}_{jk} = \left(\frac{1}{N_j}\overline{\mathbf{H}}_{j,/k}\mathbf{D}_{jk}^{-1}\overline{\mathbf{H}}_{j,/k}^{H} + \mathbf{Z}_j^{-1}\right)^{-1}, \quad (7)$$

with $\mathbf{D}_{jk} \in \mathbb{R}^{L(K-1)\times L(K-1)}$ *such that:* $\forall\ (u,v),\ 1,\dots,L$, $\mathcal{B}\left(\mathbf{D}_{jk},u,v\right) = diag\left\{\frac{1}{N_j}\mathrm{tr}\left(\mathbf{R}_{jvi}\mathbf{\Phi}_{ji}\mathbf{R}_{jui}\mathbf{Z}_j\right)\right\}_{\substack{i=1\\ i\neq k}}^{K}$. *Finally, the matrix* $\overline{\mathbf{H}}_{j,k} \in \mathbb{C}^{N\times L}$ *collects the LoS components between BS*$_j$ *and the* $k-th$ *UE of each cell in the system, i.e.* $\overline{\mathbf{H}}_{j,k} = \left[\overline{\mathbf{h}}_{j1k}, \dots, \overline{\mathbf{h}}_{jLk}\right]$*; and* $\overline{\mathbf{H}}_{j,/k}$ *is the total specular matrix of BS*$_j$*,* $\overline{\mathbf{H}}_j$*, without the above* $\overline{\mathbf{H}}_{j,k}$*.*

Proof: A proof is given in Appendix A. ∎

First, as shown in [10] Assumption 2 implies that for every UE k in cell j, the correlation matrices $\mathbf{R}_{j\ell k}$, $\ell = 1,\dots,L$, are asymptotically linearly independent. When this holds, the invertibility of $\mathbf{D}_{jk}$ holds, and thus that of $\overline{\mathbf{Q}}_{jk}$ and $\mathbf{B}_{jk} + \frac{1}{N}\overline{\mathbf{H}}_{j,k}^{\mathrm{H}}\overline{\mathbf{Q}}_{jk}\overline{\mathbf{H}}_{j,k}$ is also satisfied, as shown in [3, Appendix G]. Second, Assumption 1 is classic when analyzing massive MIMO system with correlated Rician fading. It implies in addition to the existence of intra and inter-cell LoS signals. Nonetheless, if we consider Rayleigh fading, $i.e.$, $\forall(j,\ell,k)$, $\kappa_{j\ell,k} = 0$, the SINR approximation in Theorem 1 remains valid and in fact, it can be easily shown using the block matrix inversion lemma that (6) will coincide with the result given in [3]. Most importanty, note that the provided expression in Theorem 1 is an approximation of the '$\frac{1}{N_j}-$scaled' SINR, $\frac{1}{N_j}\gamma_{jk}$ which approximates to a quantity that is strictly greater than zero. As a result, Theorem 1 asserts that, under Assumptions 1 and 2, using M-MMSE gives rise to an SINR (and thus a SE) that grows unboundedly with N_j. This outcome was demonstrated in [3] for the correlated Rayleigh fading wherein $\forall(j,\ell,k)$, $\kappa_{j\ell,k} = 0$, and is validated here by Theorem 1 for correlated Rician fading systems. In contrast, all recent studies that consider single-cell combining designs such as MRC and conventional MMSE show that these schemes are limited by pilot contamination even in Rician fading. For instance, for MRC, the authors in [8] indicate that this type of interference dissipates under two conditions: asymptotic favorable propagation, and "asymptotic spatial orthogonality" between the correlation matrix of the UE of interest $\mathbf{R}_{jjk}$, and all the other correlation matrices

This article has been accepted for publication in a future issue of this journal, but has not been fully edited. Content may change prior to final publication. Citation information: DOI 10.1109/LWC.2019.2939305, IEEE Wireless Communications Letters

related to BS_j. However, it is worth mentioning that the latter, i.e. asymptotic spatial orthogonality is unlikely to occur in practice [10] and is a much stronger condition than the linear independence (assumption 2) considered in this work. As for the classical single-cell MMSE, the work [4] demonstrates that although the interference due to pilot contamination decreases with stronger LoS signals, it is only canceled as the Rician factor grows extremely large.

In Rayleigh fading, other large-scale-fading-decoding (LSFD) techniques have been shown to provide unbounded SE as [12]. However, in this work [12], the authors use the simple MRC as a first layer decoding technique, which in Rayleigh fading, is only limited by pilot contamination. Then, this latter is thereafter mitigated through LSFD in the second layer as suggested in [12]. Nevertheless, the same cannot be entailed in Rician fading, since MRC suffers from intra and inter LoS interference in addition to pilot contamination.

In conclusion, by generating a spectral efficiency that scales with the number of antennas, and this for any level of strength of LoS, M-MMSE outperforms all conventional single-cell detectors whose performance remains limited by pilot contamination in both NLoS and LoS propagation scenarios. Additionally, the validation of the LSFD scheme [12] in Rician fading and a comparison with M-MMSE can be considered as an interesting direction for future work.

The result in Theorem 1 provides an analytical framework that can be harnessed to examine the various trends of the spectral efficiency with respect to the different elements composing the network. In this line, since we consider Rician channels throughout the network, it is relevant to examine the impact of assuming inter-cell channels with both NLoS and LoS components on the overall spectral efficiency. For the sake of simplicity, we propose to investigate this aspect through the following case study, notwithstanding that the outcomes shall be validated in the simulation section.

Case Study: Consider a system with two-cells $\{1, 2\}$ each having $K = 1$ user that use the same pilot during training. Plus, $\forall(j, \ell, k)$, let the correlation matrices $\mathbf{\Theta}_{j\ell k} = \mathbf{I}_{N_j}$, and assume favorable propagation conditions between the channels corresponding the same BS, $i.e.$ for cell 1, $\frac{1}{N_1}\overline{\mathbf{h}}_{111}^{\text{H}}\overline{\mathbf{h}}_{121} \xrightarrow[N\to\infty]{a.s.} 0$. Recalling that $\beta_{j\ell k}$ represents the large-scale fading of channel $\mathbf{h}_{j\ell k}$, plugging these settings in the SINR approximation (6) leads to the following expression:

$$\frac{\overline{\gamma}_{11}}{N_1} = \frac{\alpha_{11}\left(\alpha_{11} + \kappa_{111}\phi_{11} - \frac{\alpha_{11}\alpha_{12}}{\alpha_{12}+\kappa_{121}\phi_{11}}\right)}{\phi_{11}\left(\frac{1}{\rho} + \alpha_{11} + \alpha_{12} - \frac{\alpha_{11}^2+\alpha_{12}^2}{\phi_{11}}\right)} \tag{8}$$

such that $\alpha_{1m} = \frac{\beta_{1m1}}{1+\kappa_{1m1}}$, and $\phi_{11} = \alpha_{11}+\alpha_{12}+\frac{1}{\tau\rho}$. Therefore, the objective is to investigate the impact of κ_{121} (rician factor of inter-cell LoS link between the UE in cell 2 and BS_1) on the UL SE of cell 1. To this end, a basic derivation of (8) with respect to κ_{121}, unfolds that $\frac{\overline{\gamma}_{11}}{N_1}$ is an increasing function of κ_{121}. In other words, this result demonstrates that having a combination of diffuse and specular components in inter-cell channels is more beneficial than when such links are fully scattered. Plus, the performance gain in terms of SE is increasingly higher as these inter-cell specular signals become prevalent. Consequently, this case study unveils the following result for favorable propagation conditions. Even when the system undergoes intercell specular interference, the presence of LoS signals remains a performance enabling factor in terms of UL spectral efficiency.

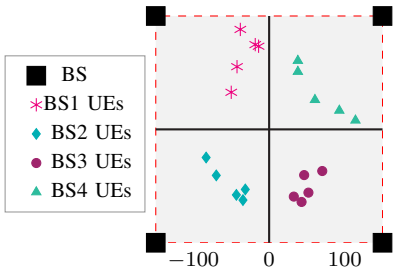

Fig. 1: $L = 4$ Multi-cell network setup with $K = 5$ UEs each.

IV. Numerical Results

We propose in this section a selection of numerical results using the $L = 4$ multi-cell setting in Fig.1 with $K = 5$ cell-edge users, and considering the exponential correlation model [13] with correlation factor 0.5. We fix $T_c = 200$ symbols, $\tau = K$, and the SNR at $-6dB$ for intra-cell UEs and between $-6.3dB$ and $-11.5dB$ for the interfering channels from other cells. For LoS channels, the specular component $[\overline{\mathbf{z}}_{j\ell k}]_n = e^{-j(n-1)\pi\sin(\theta_{jjk})}$, and each link in the system has a distinct Rician factor $\kappa_{j\ell k} \sim \mathcal{U}(0, \kappa_{\max})$. The figures illustrate the spectral efficiency, using the approximations given in Theorem 1 (dotted lines), in addition to MonteCarlo plots carried over a 1000 channel realizations (solid and dashed lines).

Fig.2 compares M-MMSE, ZF and MRC respective SEs as functions of the number of antennas. Note that both M-MMSE and ZF decoding techniques involve inversions of matrices of similar sizes and thus have fairly the same level of computational complexity. As shown, Fig.2 clearly confirms that M-MMSE outperforms both single-cell MR and ZF combining schemes for different levels of the Rician factors. Plus, as can be seen, the plots validate the accuracy of the approximations given in Theorem 1 for finite system dimensions and for different values of $\kappa_{\max}$. Since the presence of LoS links enables better SEs for both receivers as clearly depicted by the solid curves in Fig.2, we illustrate in the following its impact as "interfering inter-cell" channels. To this end, we consider in Fig.3 two scenarios of inter-cell channels, wherein case I considers both NLoS and LoS inter-cell channels ($i.e.$ $\forall(j, \ell, k)$, $\kappa_{j\ell,k} > 0$); while case II represents fully scattered inter-cell links ($i.e.$ $\forall \ell \neq j$, $\kappa_{j\ell k} = 0$). Note that the SE in this figure is plotted with respect to $\kappa_{\max}$ in order to span all ranges of practical Rician factors and ultimately highlight the impact of inter-cell specular links in all (prevailing and non-prevailing) LoS propagation environments. As can be seen, Fig.3 shows that a higher SE is achieved when the inter-cell channels are composed of both NLoS and LoS signals (solid lines as compared to the dashes ones), and this in both favorable and ordinary propagation conditions. Accordingly, Fig.3 confirms our conclusion in Section III and the case

This article has been accepted for publication in a future issue of this journal, but has not been fully edited. Content may change prior to final publication. Citation information: DOI 10.1109/LWC.2019.2939305, IEEE Wireless Communications Letters

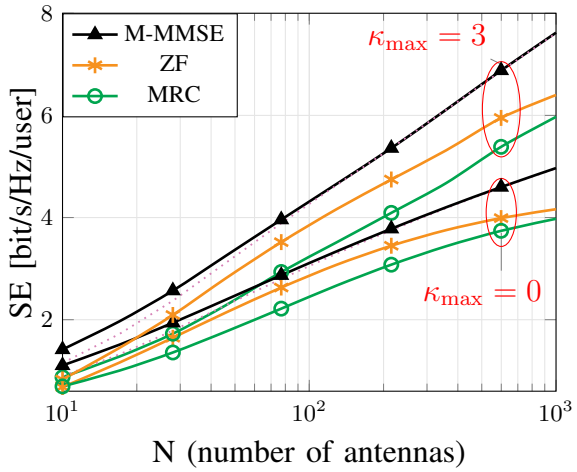

Fig. 2: UL SE using M-MMSE, ZF, and MRC with respect to the number of antennas N, for different levels of Rician factor $\kappa_{\max} \in \{0, 3\}$. Dotted lines depict the asymptotic approximation given in Theorem 1.

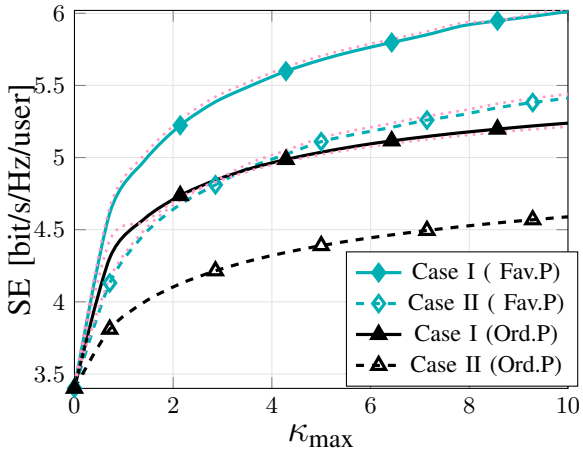

Fig. 3: UL SE using M-MMSE with respect to $\kappa_{\max}$ for $N = 200$, in both ordinanary (Ord.P) and favorable (Fav.P) propagation conditions. Case I indicates both NLoS and LoS inter-cell channels, while Case II represents fully scattered inter-cell links

study, which stated that having both NLoS and LoS inter-cell channels culminates to a better SE than when said links are fully scattered.

V. Conclusion

We analyzed in this letter the UL performance of multi-cell MMSE combining in the context of massive MIMO systems. Each channel accounts for both NLoS and LoS components with a distinct spatial correlation and Rician factor, and is subject to pilot contamination and imperfect estimation. Considering the large-antenna limit, we derived closed-form approximations of the achievable spectral efficiency. To highlight the performance gain emanating from M-MMSE, we compared this latter's SE with the classic MR combining. The analysis and numerical results confirm that M-MMSE allows unbounded UL spectral efficiency, and thus outperforms single-cell receivers such as MRC. Another key result shows that even when the LoS is present in forms of inter-cell interfering links, it remains a performance enabling-factor in terms of spectral efficiency.

Appendix A
Proof of Theorem 1

We summarize in this appendix the main steps to obtain the approximation given in Theorem 1.

First, define the following quantities:

- $\mathbf{A}_{j,/k}$ as:

$$\mathbf{A}_{j,/k} = \sum_{\ell=1}^{L} \sum_{\substack{i=1 \\ i \neq k}}^{K} \widehat{\mathbf{h}}_{j\ell i} \widehat{\mathbf{h}}_{j\ell i}^{\mathrm{H}} + (\mathbf{Z}_j)^{-1} = \widehat{\mathbf{H}}_{j,/k} \widehat{\mathbf{H}}_{j,/k}^{\mathrm{H}} + (\mathbf{Z}_j)^{-1}, \tag{9}$$

- $\widehat{\mathbf{H}}_{j,k} \in \mathbb{C}^{N \times L}$: matrix that contains all the estimates $\widehat{\mathbf{h}}_{j\ell k}$, $\forall \ell$, $\ell \neq j$, (*i.e.* $\widehat{\mathbf{h}}_{jjk}$ and all its pilot contamintors.).

Now, using the Woodburry identity followed by the block-matrix inversion lemma, we can rewrite γ_{jk} as:

$$\gamma_{jk} = \frac{1}{\left[\left(\widehat{\mathbf{H}}_{j,k}^{\mathrm{H}} \mathbf{A}_{j,/k}^{-1} \widehat{\mathbf{H}}_{j,k} + \begin{bmatrix} 0 & \mathbf{0}_{1\times(L-1)} \\ \mathbf{0}_{(L-1)\times 1} & \mathbf{I}_{(L-1)} \end{bmatrix} \right)^{-1} \right]_{jj}}. \tag{10}$$

Then, according to the CMT, deriving a deterministic equivalent for γ_{jk}(10) essentially culminates to the $L \times L$ matrix: $\widehat{\mathbf{H}}_{j,k}^{\mathrm{H}} \mathbf{A}_{j,/k}^{-1} \widehat{\mathbf{H}}_{j,k}$, whose $mn-$th entry can be rewritten using the Woodburry inverse as:

$$\frac{1}{N_j} \widehat{\mathbf{h}}_{jmk}^{\mathrm{H}} \mathbf{A}_{j,/k}^{-1} \widehat{\mathbf{h}}_{jnk} = \frac{1}{N_j} \widehat{\mathbf{h}}_{jmk}^{\mathrm{H}} \mathbf{Z}_{j,/k} \widehat{\mathbf{h}}_{jnk} - \frac{1}{N_j} \widehat{\mathbf{h}}_{jmk}^{\mathrm{H}} \mathbf{Z}_{j,/k} \widehat{\mathbf{H}}_{j,/k} \times \left(\widehat{\mathbf{H}}_{j,/k}^{\mathrm{H}} \mathbf{Z}_j \widehat{\mathbf{H}}_{j,/k} + \mathbf{I}_{L(K-1)} \right)^{-1} \widehat{\mathbf{H}}_{j,/k} \mathbf{Z}_j \widehat{\mathbf{h}}_{jnk}. \tag{11}$$

First, since $\widehat{\mathbf{h}}_{j\ell k} \sim \mathcal{CN}\left(\overline{\mathbf{h}}_{j\ell k}, \mathbf{R}_{j\ell k} \mathbf{\Phi}_{jk} \mathbf{R}_{j\ell k}\right)$, a direct application of the CMT [14] can yield an approximation of first term in (11), *i.e.*:

$$\frac{1}{N_j} \widehat{\mathbf{h}}_{jmk}^{\mathrm{H}} \mathbf{Z}_j \widehat{\mathbf{h}}_{jnk} - \left\{ \frac{1}{N_j} \mathrm{tr}\left(\mathbf{R}_{jnk} \mathbf{\Phi}_{jk} \mathbf{R}_{jmk} \mathbf{Z}_j \right) + \frac{1}{N_j} \overline{\mathbf{h}}_{jmk}^{\mathrm{H}} \mathbf{Z}_j \overline{\mathbf{h}}_{jnk} \right\} \xrightarrow[N\to\infty]{a.s.} 0. \tag{12}$$

Second, we recall that $\widehat{\mathbf{H}}_{j,/k}$ includes all the estimates $\widehat{\mathbf{h}}_{j\ell i}$, $\forall \ell$, with $i \neq k$, thus implying that it is fully uncorrelated with

This article has been accepted for publication in a future issue of this journal, but has not been fully edited. Content may change prior to final publication. Citation information: DOI 10.1109/LWC.2019.2939305, IEEE Wireless Communications Letters

$\widehat{\mathbf{H}}_{j,k}$ defined above. Consequently, we have:

$$\frac{1}{N_j}\widehat{\mathbf{h}}_{jmk}^{\mathrm{H}}\mathbf{Z}_j\widehat{\mathbf{H}}_{j,/k} - \left\{\frac{1}{N_j}\overline{\mathbf{h}}_{jmk}^{\mathrm{H}}\mathbf{Z}_j\overline{\mathbf{H}}_{j,/k}\right\} \xrightarrow[N\to\infty]{a.s.} 0, \tag{13}$$

$$\frac{1}{N_j}\widehat{\mathbf{H}}_{j,/k}^{\mathrm{H}}\mathbf{Z}_j\widehat{\mathbf{H}}_{j,/k} - \left\{\mathbf{D}_{jk} + \frac{1}{N_j}\overline{\mathbf{H}}_{j,/k}^{\mathrm{H}}\mathbf{Z}_j\overline{\mathbf{H}}_{j,/k})\right\} \xrightarrow[N\to\infty]{a.s.} 0, \tag{14}$$

where $\mathbf{D}_{jk}$ as defined in Theorem 1. Putting together the deterministic equivalents in (12)-(14) provides an approximation of $\frac{1}{N}\widehat{\mathbf{h}}_{jmk}^{\mathrm{H}}\mathbf{A}_{j,/k}^{-1}\widehat{\mathbf{h}}_{jnk}$. Finally, applying a reverse Woodburry on this deterministic equivalent leads to the expression $\frac{1}{N}\overline{\gamma}_{jk}$ given in Theorem 1, and thus concludes the proof.

REFERENCES

[1] T. L. Marzetta, "Noncooperative cellular wireless with unlimited numbers of base station antennas," *IEEE Transactions on Wireless Communications*, vol. 9, no. 11, pp. 3590–3600, November 2010.

[2] A. Ashikhmin and T. Marzetta, "Pilot contamination precoding in multi-cell large scale antenna systems," in *2012 IEEE International Symposium on Information Theory Proceedings*, July 2012, pp. 1137–1141.

[3] E. BjÖrnson, J. Hoydis, and L. Sanguinetti, "Massive MIMO has unlimited capacity," *IEEE Transactions on Wireless Communications*, vol. 17, no. 1, pp. 574–590, Jan 2018.

[4] I. Boukhedimi, A. Kammoun, and M. Alouini, "LMMSE receivers in uplink massive MIMO systems with correlated Rician fading," *IEEE Transactions on Communications*, vol. 67, no. 1, pp. 230–243, Jan 2019.

[5] Q. Zhang, S. Jin, K. K. Wong, H. Zhu, and M. Matthaiou, "Power scaling of uplink massive MIMO systems with arbitrary-rank channel means," *IEEE Journal of Selected Topics in Signal Processing*, vol. 8, no. 5, pp. 966–981, Oct 2014.

[6] L. Zhao, T. Yang, G. Geraci, and J. Yuan, "Downlink multiuser massive MIMO in Rician channels under pilot contamination," in *2016 IEEE International Conference on Communications (ICC)*, May 2016, pp. 1–6.

[7] L. Wu, Z. Zhang, J. Dang, J. Wang, H. Liu, and Y. Wu, "Channel estimation for multicell multiuser massive MIMO uplink over Rician fading channels," *IEEE Transactions on Vehicular Technology*, vol. 66, no. 10, pp. 8872–8882, Oct 2017.

[8] Ö. Özdogan, E. Björnson, and E. G. Larsson, "Massive MIMO with spatially correlated Rician fading channels," May 2018. [Online]. Available: http://arxiv.org/abs/1805.07972

[9] L. Sanguinetti, A. Kammoun, and M. Debbah, "Theoretical performance limits of massive MIMO with uncorrelated Rician fading channels," *IEEE Transactions on Communications*, vol. 67, no. 3, pp. 1939–1955, March 2019.

[10] E. Björnson, J. Hoydis, and L. Sanguinetti, "Massive MIMO networks: Spectral, energy, and hardware efficiency," *Foundations and Trends® in Signal Processing*, vol. 11, no. 3-4, pp. 154–655, 2017.

[11] P. Billingsley, *Probability and Measure*, 3rd ed. New York: Wiley, 1995.

[12] T. Van Chien, C. Mollén, and E. Björnson, "Large-scale-fading decoding in cellular massive MIMO systems with spatially correlated channels," *IEEE Transactions on Communications*, vol. 67, no. 4, pp. 2746–2762, April 2019.

[13] S. L. Loyka, "Channel capacity of MIMO architecture using the exponential correlation matrix," *IEEE Communications Letters*, vol. 5, no. 9, pp. 369–371, Sept 2001.

[14] D. Paul and J. W. Silverstein, "No eigenvalues outside the support of the limiting empirical spectral distribution of a separable covariance matrix," *Journal of Multivariate Analysis*, vol. 100, no. 1, pp. 37 – 57, 2009.